

We are IntechOpen, the world's leading publisher of Open Access books Built by scientists, for scientists

6,900

Open access books available

185,000

International authors and editors

200M

Downloads

Our authors are among the

154

Countries delivered to

TOP 1%

most cited scientists

12.2%

Contributors from top 500 universities



WEB OF SCIENCE™

Selection of our books indexed in the Book Citation Index
in Web of Science™ Core Collection (BKCI)

Interested in publishing with us?
Contact book.department@intechopen.com

Numbers displayed above are based on latest data collected.
For more information visit www.intechopen.com



Rare-Earth Doped Optical Fibers

Efraín Mejía-Beltrán
Centro de Investigaciones en Óptica
México

1. Introduction

An optical fiber becomes active by doping its core with one or more atomic elements, usually (but not restricted to) rare-earths (RE's), more specifically, the *lanthanides* that occupy the atomic numbers 57 to 71 of the periodic table. As it will be mentioned later in more detail, they use three electrons in bonding to the condensed materials such as crystals and glasses to become triply ionized ions. Because they present absorption and emission bands from UV to NIR, the materials doped with these become very active in converting the properties of optical signals. Most optical fibers are made of crystal quartz (SiO_2) that is melted and cooled down such that stays "frozen" in its vitreous state. This disordered pattern of the constituents, Silicon and Oxygen, produce randomly distorted unit cells of the crystal (quartz) to become *silica*. Other important fiber materials with special properties have been discovered (and studied) during the last decades; among the vast variety, the zirconium-fluorides (also named fluorozirconates) have been of special importance because the RE's notably change their spectral properties. Among those changes are the broadening of the absorption and emission bands and much longer excited state lifetimes of up to some orders of magnitude compared to silica. In addition, their operation region covers and further exceeds the silica transparency band (~200 to 2100 nm) to be ~200-6000 nm (Lucas, 1989). Broader absorption bands allow the use of non wavelength-stable or even multi-line delivering pumps, usually provided by the cheapest semiconductor lasers; whereas with broader emission bands, it is possible to cover a wide range of emitting wavelengths. For illumination or broadband sources this characteristic becomes important (Digonnet, 2001). Also the optical fiber amplifiers (FA's) that amplify weak signals such as the channels of telecommunication systems increase their capacity thanks to this characteristic. Because a laser is an amplifier with a resonant cavity, it is possible to take advantage of this broad emission spectrum to generate several laser lines by designing the appropriate resonator or even, it is possible to insert a wavelength selecting device within the cavity to select the desired wavelength to be emitted. This topic is described in more detail in another chapter of this book. Longer lifetimes benefits efficiency in some fiber lasers (FL's) and FA's and also increase the probability for already excited ions to absorb another photon that re-excites them to a more energetic state from which, if the lifetime is also long a third photon may be absorbed, and so on. This re-excitation is called *excited state absorption* (ESA) and when two or more photons are absorbed to excite a higher energy level capable of producing or amplifying signals of shorter wavelengths, it is said that *upconversion* occurs. This phenomenon will be sufficiently discussed later in this chapter. For now it is enough to say

that some ions inside some glasses may absorb IR signals and produce laser emissions and amplification in the VIS-UV region.

Apart from the first flash-lamp pumped FL's and FA's in which a spectral portion of the incoherent light converts into monochromatic-coherent light, FL's are strictly speaking *fiber laser converters* because they convert the coherent wavelength(s) of the laser pump into different (also coherent) ones. Because their optical-to-optical conversion efficiencies range from 5 to >95%, FL's are among the most efficient lasers.

In order to illustrate the advantages of typical fiber-based devices compared to their bulk counterparts, let us depart from the following example. In typical solid-state laser-pumped lasers such as the Nd³⁺:YAG or Ti:Sapphire, the active length of the laser material is at most few centimeters. Just to give an idea of this, let us suppose that we have a single-mode (SM) 2mm-diameter collimated gaussian beam from a 808-nm laser to pump a Nd³⁺-doped glass laser. If we want to produce a 6- μm beam waist ($2w_0$) in the middle of the glass, an 11.7 mm focal length lens would be necessary as illustrated in Figure 1.

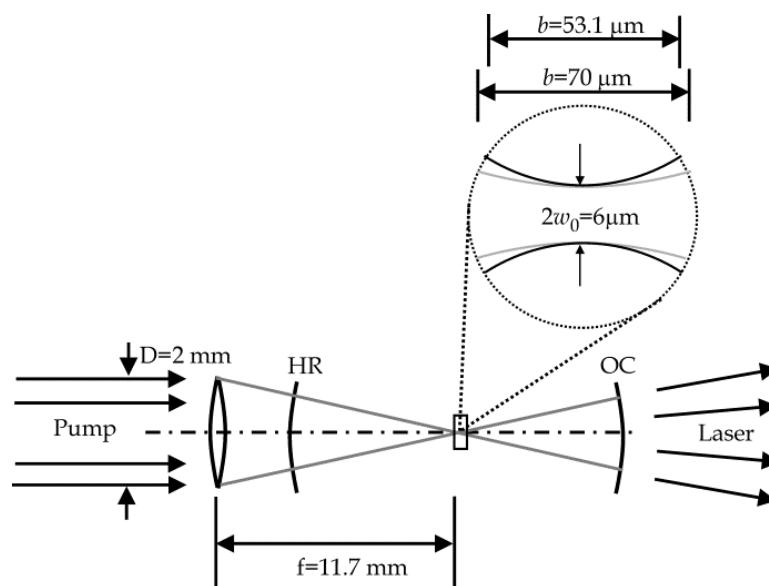


Fig. 1. Typical scheme of a bulk laser.

The region in which the beam is practically collimated is called the confocal parameter that gives $b\sim 70\mu\text{m}$ (Siegman, 1986). An active cavity for the laser signal desired, 1064 nm for example, may be formed by using two mirrors; a high reflector (HR) and an output coupler (OC). The curvatures of the mirrors, the distance between them and the position of the active material have to be such that the lowest order gaussian mode of the 1064-nm signal is perfectly confined inside the cavity. The confocal parameter for this signal with the same beam waist is different than the one for the pump and gives $b\sim 53.1\mu\text{m}$ meaning that the spatial overlap between both beams is partial. Larger active volumes are achieved by increasing the beam waists; however, this implies to use very large focal lengths for the lenses. For example for a $\sim 100\text{-}\mu\text{m}$ waist, $f\sim 19.4\text{ cm}$ and $b\sim 19.4\text{ mm}$; with these values the system is reaching the limit of being compact. The focused pumping beam in larger systems might be "bended" by using mirrors but a new issue appears because the larger active volume produces more heat that needs to be dissipated and a cooling system is required. Apart from these differences, larger beam waists imply higher pump power to

reach laser operation because energy density within the active volume decreases. Then, larger systems are appropriated for non-compact high-power lasers. In our 6- μm waist example, low operating threshold in the order of tens of milliwatts, no cooling requirements for power delivery in the order of ~ 100 mW and low power delivery are possible. Even supposing that the concentration of dopants is the right one, pump absorption by such a short sample would be very inefficient because absorption also depends on length. In order to assure the oscillation of the cavity with such a tiny active region, the reflectivities of both mirrors would be close to 100 % because lower reflectivities means high cavity loss to overcome by the cavity gain. Let us say that the high reflector (HR) is 100 % and the output coupler (OC) has 99%. In this way, it will only deliver 1% of the signal generated inside the cavity. In addition to that, the glass surfaces may need anti-reflection coating to reduce loss from the air-glass interfaces. This would be an inefficient system delivering $<1\%$ of the total signal generated by the cavity, i.e. less than 1mW for 100 mW pump power. Any attempt to extract more power, let's say replacing the OC to 95 % to produce ≤ 5 mW, would most possibly lead to: a) no oscillation at all, b) oscillation with very unstable behavior or c) higher pump power threshold for oscillation. Let us now introduce some changes to our system. Suppose the replacement of the glass bulk by a 6- μm core Nd³⁺-doped optical fiber as in Figure 2, the mirrors attached (or deposited) at the fiber flat ends, and the pump signal focused at one end (the HR transparent for this signal). Now we have a sufficiently large material that more efficiently absorbs the pump and has a larger gain length (usually from tens of cm to hundreds of meters) with a total overlap of the beams. In such high-gain cavity, it is possible to change the OC to extract more than 50 % of the optical power. These changes briefly describe the upgrade from conventional bulk lasers to RE-doped fiber lasers (REDFL's). Coiled optical fibers mean much larger fiber-cavities occupying a modest space. Apart from being very stable, FL's that deliver up to some watts, easily connect to a fiber-link and most have an excellent, usually circular, beam quality. The enlarged active volume (the fiber core) is in the center of a fine glass strand (the optical fiber) and because the ratio of the fiber surface to the active volume is immense the heat produced in the active volume easily dissipates through the large surface. This makes these systems not to require cooling systems when delivering up to some watts. These unique characteristics make them among the best candidates for the development of new laser sources. In fact, the limitations of laser diodes, such as low power and poor beam quality were overcome by the invention of the double-cladd optical fiber (Po et al., 1989). On that guiding structure, the low-quality pump-beam provided by an array of laser diodes couples into a very large core (up to 125 microns and sometimes non-circular) and as it propagates, it pumps the single-mode RE-doped core (usually at the center). The single-mode signals emitted by such multimode-excited core preferentially amplify along its axis. In this way, the low quality beam transforms into a high-quality one.

Most recent applications of RE-doped fibers (REDF's) include temperature sensors and optically-controlled fiber attenuators (OCFA's). Concerning temperature sensors, a REDF is optically pumped to excite certain transition whose upper energy level has a close lower-energy one. At low temperatures, the atomic vibrations of the glass weakly (non-radiatively) de-excite ions from the upper to the lower-energy one. At room temperature the ions from both levels directly decay to a much lower energy level, the ground state for example; in doing so they release the corresponding photons that form two bands whose peak

wavelengths are very close. A temperature increase increases the non-radiative vibration-induced transitions that change the shape of the optical spectrum emitted; the emitted higher-energy photons decrease while the lower-energy ones increase. The intensity ratio of these bands becomes proportional to temperature values (Castrellón-Urbe & García-Torales, 2010). Advantages of this type of sensor include non-electrical and remote operation because a large optical fiber guides the pump signal to the transducer (the doped fiber) and also collects the signals to be processed. OCFA's consist on guiding a non ground-state resonant-signal. This probe signal becomes absorbed by co-guiding a control signal that excites the ions from the ground state to a excited state that activates the absorption of the probe (Mejia & Pinto, 2009). This device will be detailed later in the chapter.

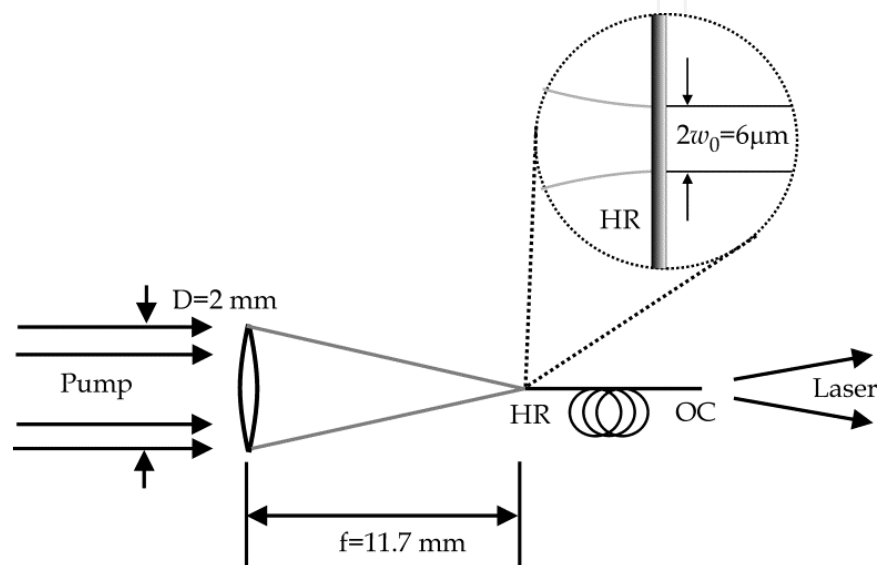


Fig. 2. Fiber laser.

2. Principles of operation

In this section, the electronic configuration of the rare earths becomes the natural departing point that allows understanding the light-matter interactions. Because the optical fibers are usually made of glass, these interactions change slightly depending of the type of glass they are immersed in. The basic pumping schemes that exist to produce light amplification are described and qualitatively compared, being described more quantitatively in the next section. Also an important phenomenon called upconversion in which the production of high energy photons are produced by the absorption of two or more lower-energy ones is described and its special qualities highlighted. The most general and basic formulas that are common to all the fiber devices covered in the chapter are obtained here.

2.1 Triply ionized rare-earths as active centers

As mentioned before, the lanthanides have atomic numbers from 57(La) to 71(Lu). When immersed in glass, three of their electrons are used in bonding to the glass-molecules, two from the s-type orbital of the outer ($n=6$) shell, and one from an f-type orbital of an inner shell ($n=4$). The absence of those negative charges, unbalances the atomic charge to $3+$ because the number of protons in the nucleus do not vary. Thus, it is said that the RE atoms become triply ionized when immersed in glass. This ionization changes their electron

configuration to be equivalent to the elements in the periodic table that are three places below concerning atomic number (Z). For example, Lanthanum (La) that has 57 electrons ($Z=57$) in its neutral state, becomes La^{3+} with the electron configuration of Xe ($Z=54$): $1s^2 2s^2 2p^6 3s^2 3p^6 4s^2 3d^{10} 4p^6 5s^2 4d^{10} 5p^6$. In words, this electron configuration may be described as: "two electrons are in the first shell occupying the simplest type of orbital ($1s^2$); eight in the second shell, two occupying the s-type orbital or sub-shell ($2s^2$) and the rest in the other sub-shell that is composed of three, more complex in shape and hence more energetic p-type orbitals that are orthogonally-oriented and allocate two electrons each ($2p^6$); and so on..." From all, only La^{3+} and Lu^{3+} have all the sub-shells completely filled (or closed); their electron configurations are $(\text{Xe})4f^0$ and $(\text{Xe})4f^{14}$ respectively; this makes them optically inactive because there are no vacant sites (quantum states) in the orbitals within the f sub-shell that might temporarily allocate optically-excited electrons from other orbitals i.e. it is not possible to temporarily change the electron arrangement. In contrast, all others from $\text{Ce}^{3+}[(\text{Xe})f^1]$ to $\text{Yb}^{3+}[(\text{Xe})f^{13}]$ have quantum states "available" within the non-closed f sub-shell. On these, the non-occupied f -type orbitals may be temporarily occupied by optically-excited electrons coming from lower energy orbitals. In short, energy changes of the ions are produced by electronic re-arrangements within the $4f$ sub-shell. These transitions are relatively unaffected by external perturbations such as electro-magnetic fields and vibrations from the host material because the most external $5s$ and $5p$ closed sub-shells produce a *shielding effect*. According to Pauling (Pauling, 1988) the atoms with higher Z have their inner shells closer to the nucleus because of the increase of charge (more protons and electrons). Since the $4f$ sub-shell is physically closer to the nucleus than the $5s$ and $5p$, they become more compact and thus more protected as Z increases. Then, the $4f$ electronic transitions of Ce^{3+} are more influenced by the glass perturbations than those of the one with the highest atomic number, Yb^{3+} . Without excitation, a RE ion stays in its more stable electron arrangement called the ground state (GS) that has the energy that corresponds to the vector superposition of all the quantum states of the electrons (Miniscalco, 2001). Changes in the electron arrangement means changes of energy of the ions, then, the number of energy levels that one ion can take when excited depends on the number of electron sites available. For example, Yb^{3+} that has only one quantum state available can be in one of two possible energies, the GS or the excited state (ES). Before describing more complicated sets of levels that correspond to the rest of RE's let us briefly describe the origin of the energy intrinsic to an atom.

As established by quantum mechanics, each electron has a unique set of quantum numbers n , l , m and s that quantify its energy and position within an atom. The first one describes the radial region (number of shell) in which it stays most of the time regardless of its orbital movement. The second quantum number indicates the number of units of angular momentum that is proportional to the magnetic field produced by its movement and as such, it depends on the type of orbital (also called sub-shell); the s-type corresponds to $l=0$ because its shape is simply spherical, the p -type corresponds to the lowest angular momentum ($l=1$) because it has a slightly more complex shape; with even more "exotic" shapes are d and f with $l=2$ and $l=3$ respectively. The s-type sub-shell has a pair of electrons occupying a single orbital; the p -type has three pairs occupying three orbitals; the d five, and the f seven. Within a sub-shell, the orbitals have in general the same shape (l) but differ in spatial orientation (m). Then the vector of angular momentum composed of magnitude (l) and direction (m) of the translational movement of the electron is complete. The fourth quantum number (s) refers to the vector that describes the magnetic field produced by the

electron's rotation on its axis and it is called the *spin* number. Then, the two electrons that occupy a specific orbital rotate in opposite directions (Pauling, 1988).

As mentioned before, without excitation a RE³⁺ keeps its most stable energy, the GS which is given by the natural arrangement of the electrons in the 4*f* orbitals. Any re-arrangements of these electrons by excitation cause discrete energy changes. The orbital angular momentum vectors of all the individual 4*f*-electrons may be added to form a resultant vector (**L**) and in the same manner, the vector addition of their spins gives **S**, being the total angular momentum $\mathbf{J}=\mathbf{L}+\mathbf{S}$; this is called the Russell-Saunders or spin-orbital coupling. Because every electron arrangement has its own **JLS** set of values, the possible energy values are labeled accordingly as ^{2S+1}L_J (Miniscalco, 2001). The possible values of **L** are given by the letters S, P, D, F, G, H, I, K..., that correspond respectively to 0, 1, 2, 3, 4, 5, 6, 7.... In this way, the labeling of the energy levels commonly used in the literature make sense because the superscript on the left gives information of the spins, the letter that corresponds to **L** gives information of the orbitals that are occupied and **J** is a combination of both.

2.2 Optical properties of RE-doped glasses

In spite of the shielding of the 4*f* transitions, when the RE ions are introduced as dopants in condensed materials such as crystals or glasses, weak interactions with the electrostatic field of the atomic arrangement take place and as a consequence each **JLS** level split into discrete sub-levels (called multiplet) because of the weak electrostatic interactions with the atoms of the material. This is called the Stark effect and it is so weak that the sub-levels are spaced between 10 and 100 cm⁻¹. The strength of the effect depends on the type of host material, and in most materials their broadening produces overlap due to the material vibration (temperature). Then, except for very low (close to cryogenic) temperatures, the net effect is a band creation whose width depends on the host material. Because in crystals all the atoms of the network are perfectly ordered, all the RE ions are affected by identical fields and it is said that they are *homogeneously broadened*. Glasses by contrary have site-to-site field variations because their atoms are not as ordered as in crystals and hence each ion has its own multiplet. This is called *inhomogeneous broadening* and even in a small sample the overlap of all the multiplets creates bands whose widths depend on the type of glass. The optical properties of the RE's immersed into two very different type of glasses are described right away.

In general, most optical fiber glasses used as hosts for RE's have optical properties between the silica and fluorozirconates from which the most common is the ZBLAN that owe its name to its constituents ZrF₄, BaF₂, LaF₃, AlF₃ and NaF. Each glass responds different to temperature that manifests as vibrations because of its molecular composition. For example, the superposition of all the possible vibrational energies (phonons) for silica form a continuum that covers a band of 40 THz ($\lambda_{\text{phonon}} \geq \sim 7.5 \mu\text{m}$, $\Delta E \leq 1300 \text{ cm}^{-1}$) with the strongest mode overlapping at $\sim 7.5\text{-}15.5 \text{ THz}$ that corresponds to 19.35 and 40 μm ($250 \leq \Delta E \leq 520 \text{ cm}^{-1}$), respectively (Agrawal, 1989). By contrast, a fluoride-based glass, ZBLAN for example, presents a much narrower band with mode overlapping at the edge 15 THz that corresponds to $\lambda_{\text{phonon}} \sim 20 \mu\text{m}$ ($\Delta E \approx 580 \text{ cm}^{-1}$) (Luu-Gen & Chen-Ke, 1996; Quin et al. 1997). Then, all the energy levels separated less than this GAP, 1300 cm⁻¹ for silica and 580 cm⁻¹ for ZBLAN, are thermally connected and the higher instantaneously feeds population into the lower. Because the phonon spectrum of ZBLAN is narrower, two levels thermally connected in Silica, may not be alike in ZBLAN; then, more radiative transitions are possible in ZBLAN.

2.3 Three and four-level pumping schemes for light amplification

The most important pumping schemes for fiber amplifiers and lasers depend on the energy level arrangement of the ions in the glass. In general, they can be classified as four or three-level systems (Fig. 3). In real systems there may be many more levels involved in, but they can be simplified to either of these as follows. Fig. 3(a) shows the four-level scheme. Without any excitation, all the ions are in the ground state E_1 with a total density N_1 . When exciting with the wavelength that corresponds to the energy difference between E_1 and E_4 , part of the ions populate E_4 from where they decay very rapidly down to E_3 by releasing phonons because E_4-E_3 lies within the energy vibrations of the glass. Hence, the level E_4 may be considered as practically empty because it does not retain ions, they just pass through it to populate E_3 (density N_3) where they tend to accumulate because this level is not vibration-connected to E_2 and hence the only way to decay is by an emission of the corresponding E_3-E_2 photons. The ions stay for a short time in E_3 which produces energy accumulation. This level is called the *metastable level* and typical lifetime values are from tens of microseconds to some milliseconds and depend on the type of glass.

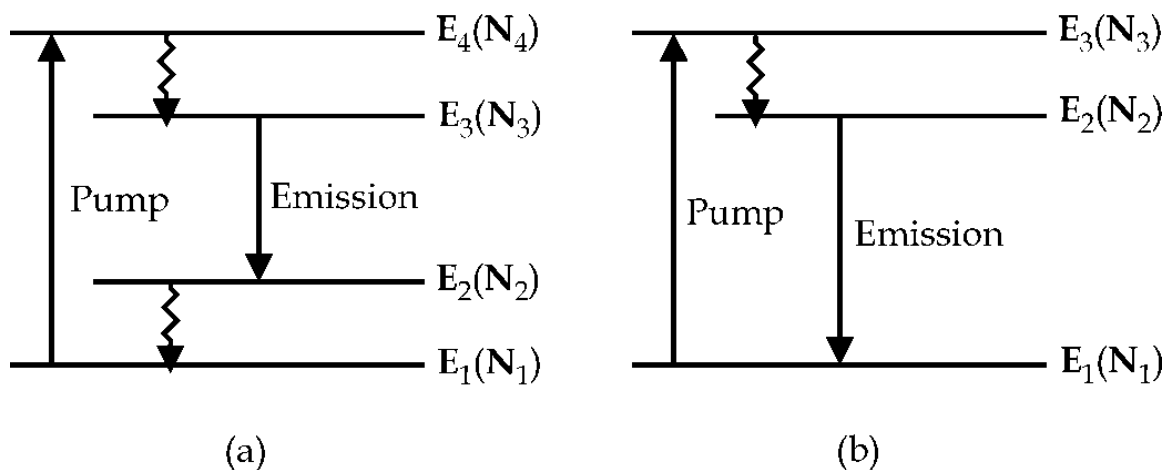


Fig. 3. (a) Four-level pumping scheme (b) Three-level pumping scheme.

Certain level of a RE may exhibit a lifetime more than one order of magnitude in ZBLAN (or other low-energy phonon glass) than its lifetime in silica for example. As the ions make the transition to E_2 , spontaneously emit the corresponding photons and from this level that is also thermally connected to the ground state they instantaneously decay to the ground state by providing energy vibrations to the glass (phonons). Thus, E_2 does not accumulate population ($N_2 \approx 0$) similar to E_4 ($N_4 \approx 0$) and as a consequence it is possible to obtain population inversion ($N_3 \gg N_2$). Under this condition, the spontaneously-emitted photons of energy E_3-E_2 propagate mostly through excited ions on E_3 and because of resonance with E_3-E_2 , they become "negatively absorbed" by stimulating ions from E_3 to make transitions to the practically empty E_2 . Negative absorption means stimulated emission in which one photon generates an identical one and hence optical amplification takes place because these two produce four, and so on. The signal produced in this way and that amplifies through a long material such as an optical fiber is called amplified spontaneous emission (ASE). Also an external signal of energy E_3-E_2 becomes amplified as it propagates through the fiber, this is the principle of the optical amplifiers. Also, two cavity mirrors may be placed such that they "see" each other through the fiber and reflect the E_3-E_2 signal that as it goes and returns becomes amplified, the signal that could be extracted from such cavity is the laser signal.

Apart from being easy to achieve population inversion, if part of active material (doped fiber in this case) is not excited, no signal re-absorption occurs because the E_2 - E_3 absorbing transition is inactive. Then, unlike three level systems, the optical fiber can be longer than necessary without inducing losses other than those produced by the glass (usually negligible).

Fig. 3(b) shows the three-level scheme. Here, the pumping transition is E_1 - E_3 and fast nonradiative relaxations accumulate the population on E_2 . Observe that the active transition here is E_2 - E_1 and then, if part of fiber is not excited, signal re-absorption occurs because the high density of ions in the ground state (E_1) excite to E_2 . Then, unlike four level systems, three level systems present higher pump threshold because not only the entire fiber should be excited but all the fiber should be sufficiently excited to present population inversion; otherwise, considerable loss occurs and reaching the pump threshold for lasing becomes harder. Then, in these systems, there exists an optimal fiber length for each pump power level (as studied in the next section) whereas in the four-level case, the fiber may exceed the required length. One important advantage of three-level is: less fiber heating because there is only one step of non-radiative relaxation that implies an improvement of the conversion efficiency.

2.4 Population dynamics of a three-level system

Several amplifiers and fiber lasers that have been developed are modeled as three-level systems. Among these are the transition ${}^2F_{5/2}$ - ${}^2F_{7/2}$ of Yb^{3+} , the ${}^4I_{13/2}$ - ${}^4I_{15/2}$ of Er^{3+} , the 3H_4 - 3H_6 of Tm^{3+} and the 5I_6 - 5I_8 of Ho^{3+} . All these pumping schemes have in common that the pump level is composed of at least two very close bands as shown in Figure 4(a) for Ho^{3+} in ZBLAN glass. Figure 4(b) shows an equivalent energy level diagram that represents such schemes.

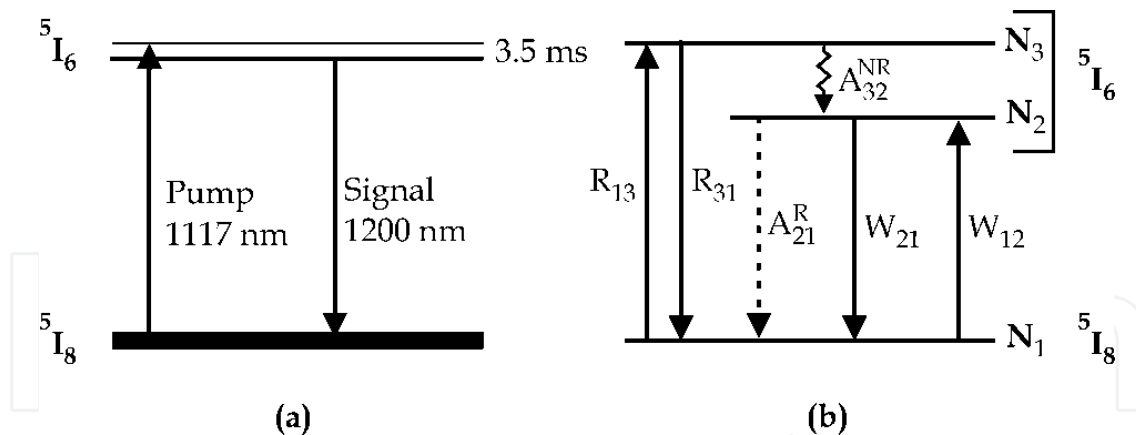


Fig. 4. (a) Partial energy level diagram of Ho^{3+} in ZBLAN glass (b) Three-level equivalent scheme.

Based on the equivalent scheme, R_{13} and R_{31} are respectively the rates of excitation and de-excitation of the pump level, their formulae are

$$R_{13} = \frac{I_p \sigma_a(\lambda_p)}{h\nu_p} \quad (1)$$

$$R_{31} = \frac{I_p \sigma_e(\lambda_p)}{h\nu_p} \quad (2)$$

W_{12} and W_{21} are the ones corresponding to the signal

$$W_{12} = \frac{I_s \sigma_a(\lambda_s)}{h\nu_s} \quad (3)$$

$$W_{21} = \frac{I_s \sigma_e(\lambda_s)}{h\nu_s} \quad (4)$$

$$A_{21} = \frac{1}{\tau_{21}} \quad (5)$$

And the latter refers to the radiative ratio where τ_{21} is the 5I_6 level lifetime.

With pump and generated signal varying, the ions dynamically distribute on the energy levels as [From Fig. 4(a)]

$$\frac{dN_1}{dt} = -N_1(W_{12} + R_{13}) + N_2(A_{21}^R + W_{21}) + N_3R_{31} \quad (6)$$

$$\frac{dN_2}{dt} = -N_2(A_{21}^R + W_{21}) + N_1W_{12} + N_3A_{32}^{NR} \quad (7)$$

$$\frac{dN_3}{dt} = -N_3A_{32}^{NR} + N_1R_{13} \quad (8)$$

$$N_t = N_1 + N_2 + N_3 \quad (9)$$

The last one refers to the energy conservation law, NR to non-radiative and N_t is the RE concentration. Solving this system of equations by supposing CW signals (i.e. the $dN's/dt=0$) one may obtain the population densities at each level. Another equation is added for a four-level system, and so on. However, in the system treated here, simplifications may be realized. With the arguments of section 2.3 and the fact that in the RE's mentioned the absorption and emission bands overlap as shown for Ho^{3+} in Figure 5(a), the system may be reduced to a two-level one with $N_3 \approx 0$ (very high A_{32}^{NR}) and including the R 's within the W 's with the right changes [see Fig. 5(b)]. Then Equations (3) and (4) change to

$$W_{12} = \frac{I_p \sigma_a(\lambda_p)}{h\nu_p} + \frac{I_s \sigma_a(\lambda_s)}{h\nu_s} \quad (10)$$

$$W_{21} = \frac{I_s \sigma_e(\lambda_s)}{h\nu_s} + \frac{I_p \sigma_e(\lambda_p)}{h\nu_p} \quad (11)$$

And hence the ions dynamically distribute on the energy levels as

$$\frac{dN_1}{dt} = -N_1W_{12} + N_2(A_{21}^R + W_{21}) \quad (12)$$

$$\frac{dN_2}{dt} = -N_2(A_{21}^R + W_{21}) + N_1W_{12} \quad (13)$$

That under CW operation become

$$N_1W_{12} = N_2(A_{21}^R + W_{21}) \quad (14)$$

$$N_2(A_{21}^R + W_{21}) = N_1W_{12} \quad (15)$$

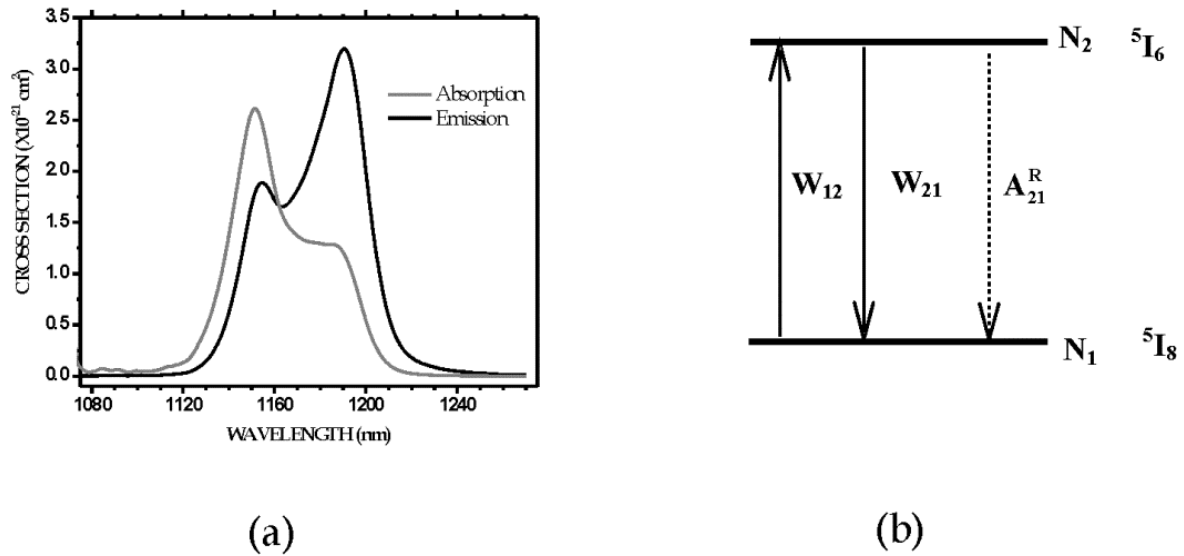


Fig. 5. (a) Measured spectra of Ho³⁺ in ZBLAN glass (b) Two-level simplified scheme.

With the energy conservation law

$$N_t = N_1 + N_2 \quad (16)$$

From these equations and equation (5) one obtains

$$N_1 = N_t \frac{1 + W_{21}\tau}{1 + W_{21}\tau + W_{12}\tau} \quad (17)$$

$$N_2 = N_t \frac{W_{12}\tau}{1 + W_{21}\tau + W_{12}\tau} \quad (18)$$

These are the population densities at each energy level of our simplified system.

2.5 Propagation equations for pump and signal

Let us suppose that a REDF operating as a quasi two-level system as mentioned in section 2.4 guides the pump beam with power P_p . The pump variation when traveling from point to point along the fiber is

$$\frac{dP_p}{dz} = [-N_1\sigma_a(\lambda_p) + N_2\sigma_e(\lambda_p)]P_p \quad (19)$$

Where

$$g_p = -N_1\sigma_a(\lambda_p) + N_2\sigma_e(\lambda_p) \quad (20)$$

Is the *gain coefficient* produced by the dopants that in most conditions is dominated by the first term being a negative gain. In the same manner, it is possible to establish that for the propagating signal

$$\frac{dP_s}{dz} = [N_2\sigma_e(\lambda_s) - N_1\sigma_a(\lambda_s)]P_s \quad (21)$$

Where

$$g_s = N_2\sigma_e(\lambda_s) - N_1\sigma_a(\lambda_s) \quad (22)$$

Refers also to the gain coefficient.

When the fiber is not pumped and a weak signal propagates, $N_2 \approx 0$ and hence all the population is at the ground state ($N_1 = N_t$), $g_p \approx -N_1\sigma_a(\lambda_p)$ and then the "gain coefficient" becomes the *small signal loss coefficient* as

$$\alpha_0 = N_t\sigma_a(\lambda) \quad (23)$$

The loss coefficient is a function of the pump power (or intensity) as follows (Siegman, 1986)

$$\alpha(P_p) = \frac{\alpha_0}{1 + \frac{P_p}{P_p^{sat}}} \quad (24)$$

And for transitions in which there is not spectra overlap $P_p^{sat} = \frac{h\nu_p a}{\sigma_a \tau}$ is the pump power that makes possible to have $\alpha = \frac{\alpha_0}{2}$ and obviously it is called the *saturation pump power*; here a is the cross section area of the fiber core. Hence, a definition for the *saturation intensity* is $I^{sat} = h\nu/\sigma\tau$.

Establishing a *small signal gain coefficient* is more complicated because it depends on the population distribution. It is better to say that under population inversion conditions a weak signal that do not notably redistributes the population experiences a small signal gain; whereas more powerful signals that redistribute population tend to experience less gain. Then

$$g(P_s) = \frac{g_0}{1 + \frac{P_s}{P_s^{sat}}} \quad (25)$$

With $P_s^{sat} = \frac{h\nu_s a}{\sigma_e \tau}$ as the *saturation signal power*. For quasi two-level systems (Desurvire, 1994) these saturation signal equations are

$$P_p^{sat} = \frac{h\nu_p a}{[\sigma_a(\lambda_p) + \sigma_e(\lambda_p)]\tau} \quad (26)$$

$$P_s^{sat} = \frac{h\nu_s a}{[\sigma_a(\lambda_s) + \sigma_e(\lambda_s)]\tau} \quad (27)$$

The ratio emission-to-absorption cross sections at λ_s or λ_p may be defined as

$$\eta_i = \frac{\sigma_e(\lambda_i)}{\sigma_a(\lambda_i)} \quad i = s, p \quad (28)$$

That introduced in (26) and (27) makes them

$$P_p^{sat} = \frac{h\nu_p a}{[1 + \eta_p]\sigma_a(\lambda_p)\tau} = \frac{\eta_p h\nu_p a}{[1 + \eta_p]\sigma_e(\lambda_p)\tau} \quad (29)$$

$$P_s^{sat} = \frac{h\nu_s a}{[1 + \eta_s]\sigma_a(\lambda_s)\tau} = \frac{\eta_s h\nu_s a}{[1 + \eta_s]\sigma_e(\lambda_s)\tau} \quad (30)$$

Because $P = I a$ and multiplying (10) and (11) by τ , they become

$$W_{12}\tau = \frac{P_p\sigma_a(\lambda_p)\tau}{h\nu_p a} + \frac{P_s\sigma_a(\lambda_s)\tau}{h\nu_s a} \quad (31)$$

$$W_{21}\tau = \frac{P_s\sigma_e(\lambda_s)\tau}{h\nu_s a} + \frac{P_p\sigma_e(\lambda_p)\tau}{h\nu_p a} \quad (32)$$

Solving (29) and (30) for $\sigma\tau/h\nu a$ and normalizing signal powers as

$$p = \frac{P_s}{P_s^{sat}} \text{ and } q = \frac{P_p}{P_p^{sat}} \quad (33)$$

(31) and (32) in a normalized version are

$$W_{12}\tau = \frac{1}{[1+\eta_s]}p + \frac{1}{[1+\eta_p]}q \quad (34)$$

$$W_{21}\tau = \frac{\eta_s}{[1+\eta_s]}p + \frac{\eta_p}{[1+\eta_p]}q \quad (35)$$

Also using (28), the propagation equations (19) and (21) may be expressed as

$$\frac{dP_p}{dz} = \sigma_a(\lambda_p)[\eta_p N_2 - N_1]P_p \quad (36)$$

$$\frac{dP_s}{dz} = \sigma_a(\lambda_s)[\eta_s N_2 - N_1]P_s \quad (37)$$

Where the populations N_1 and N_2 are now expressed as [introducing (34) and (35) in (17) and (18)]:

$$N_1 = N_t \frac{1 + \frac{1}{1+\eta_s}p + \frac{1}{1+\eta_p}q}{1+p+q} \quad (38)$$

$$N_2 = N_t \frac{\frac{1}{1+\eta_s}p + \frac{1}{1+\eta_p}q}{1+p+q} \quad (39)$$

That introduced in the propagation equations give

$$\frac{dP_p}{dz} = -\sigma_a(\lambda_p)N_t \frac{1 + \frac{\eta_s - \eta_p}{1+\eta_s}p}{1+p+q} P_p \quad (40)$$

$$\frac{dP_s}{dz} = \sigma_a(\lambda_s)N_t \frac{\frac{\eta_s - \eta_p}{1+\eta_p}q - 1}{1+p+q} P_s \quad (41)$$

Using the definition for the small signal loss [equation (23)], normalizing to the saturation powers, defining $U' = \frac{\eta_s - \eta_p}{1+\eta_s}$ and $U = \frac{\eta_s - \eta_p}{1+\eta_p}$; the propagation equations reduce to

$$\frac{dq}{dz} = -\alpha_p \frac{U'p+1}{1+p+q} q \quad (42)$$

$$\frac{dp}{dz} = \alpha_s \frac{Uq-1}{1+p+q} p \quad (43)$$

3. Fiber lasers

In 1960, while working for the Huges Research Laboratory in California, T. H. Maiman reported on August the first laser by irradiating (pumping) a crystal (ruby)-cavity with a powerful flash lamp.¹ Soon after, on December 1961, while working for the American

Optical Company in Massachusetts, E. Snitzer reported laser oscillation in an optical fiber based cavity.² It consisted of a Nd³⁺-doped optical fiber cavity pumped by a flash lamp that for obvious reasons was termed *fiber laser* (FL). The fact that absorption losses in optical fibers were gradually decreasing (at present for example the best telecommunication fibers have a loss of less than 0.2 dB/km), together with the development of semiconductor lasers that were introduced as pumps for this type of lasers strongly motivated its investigation that boomed in the 1980's. Laser diodes are among the most efficient with typical overall electrical-to-optical conversion efficiencies superior to 50 %.

The pumping signal excites the atoms of the medium into a higher energy level to create population inversion that means amplification and therefore lasing. The pump is usually provided by another laser. In the work described here, the pump source was a diode-pumped fiber laser system operating at 1064-nm wavelength and the active material was an Ho³⁺-doped optical fiber.

The optical cavity is created by two mirrors arranged such that the light amplifies as it travels back and forth through the gain medium. Regularly one of the two mirrors (the output coupler) is partially transparent with the purpose that part of the signal is emitted through it. These mirrors can be dichroic filters, Bragg gratings or simply perpendicular cleaved facets of fiber-ends. In the later, highly efficient lasers only require the ~4% of the amplified signal to travel back into the cavity to be re-amplified and the rest (96%) is delivered as useful laser light.

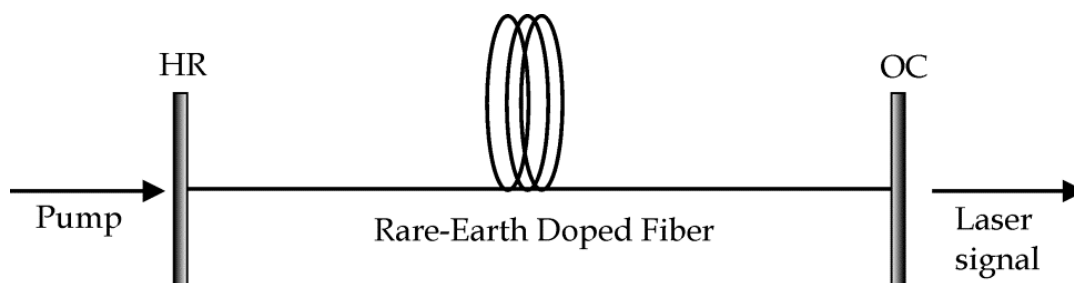


Fig. 6. Typical configuration of a fiber laser. The mirror **HR** has high transmission for the pump wavelength (λ_p) and high reflection for the laser signal (λ_s); the mirror **OC** partially reflects λ_s and the transmitted part is the laser signal.

3.1 Modeling of a quasi two-level fiber laser

As introduced on section 2, three-level pumping amplifying systems may be studied as quasi two-level when absorption and emission spectra overlap. Because these systems need to present population inversion all along the optical fiber, a serious level of pump power is not absorbed and hence emitted as residual. This is a serious limitation of these systems concerning optical conversion efficiency. However, in order to assure that most of the absorbed power transfers to the amplifying signal, an optimal length needs to be estimated. This is our goal in this section.

Along a fiber laser there are two stimulated-emission generated signals that propagate in opposite directions. Figure 6 depicts these signals together with the pump from zero to the optimal fiber length (L_{opt}). The total (normalized) power at any point (z) is

$$p(z) = \beta^+(z) + \beta^-(z) \quad (44)$$

Where

$$\beta^+(z) = \frac{P_s^+(z)}{P_s^{sat}} \quad (45)$$

Propagates from the pump end ($z=0$) to the delivery end ($z=L_{opt}$) and

$$\beta^-(z) = \frac{P_s^-(z)}{P_s^{sat}} \quad (46)$$

Using equation (43) for the forward propagating signal we may write

$$\frac{1}{\beta^+} \frac{d\beta^+}{dz} = \alpha_s \frac{Uq-1}{1+p+q} \quad (47)$$

In forward pumping, the propagation equation for the pump signal is [from equation (42)]

$$\frac{1}{q} \frac{dq}{dz} = -\alpha_p \frac{U'p+1}{1+p+q} \quad (48)$$

The ratio of the propagation equations gives

$$(\alpha_p U'p + \alpha_p) \frac{d\beta^+}{\beta^+} = (-\alpha_s Uq + \alpha_s) \frac{dq}{q} \quad (49)$$

Before integrating this equation let us establish the limits. For now the left part is from $\beta^+(0)$ to $\beta^+(L_{opt})$ whereas the ones for the right part may be obtained under the criterion (see Figure 7): at $z=0$ the power is q_0 but at $z=L_{opt}$ the gain saturates and hence β^+ stops growing up. This condition makes $d\beta^+/dz = 0$ in equation (47) for $q = 1/U$ and is the key criterion for optimal performance. Integrating (49) we obtain

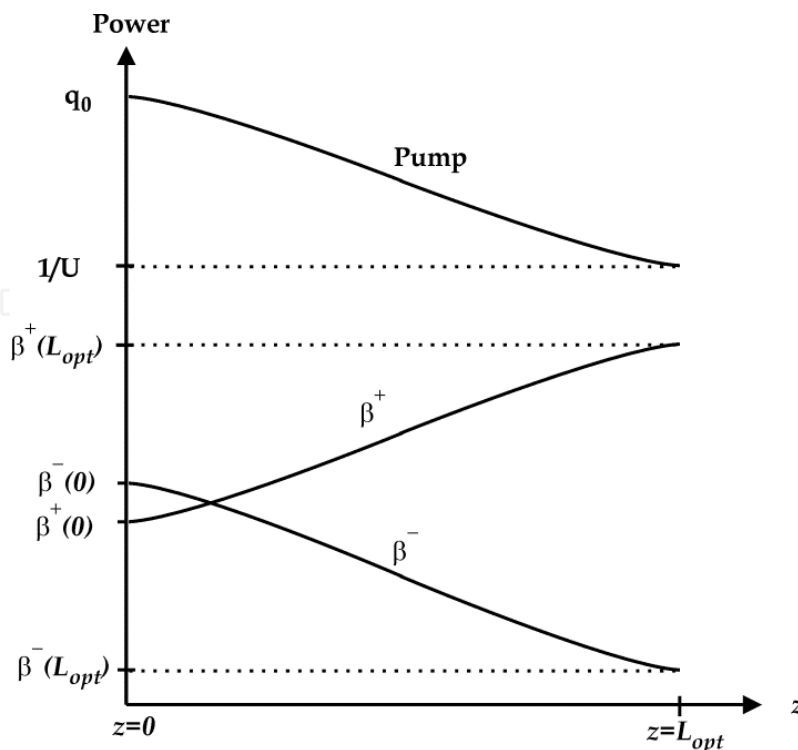


Fig. 7. Normalized powers of propagating signals along a quasi two-level fiber laser.

$$\alpha_p U' p \ln \frac{\beta^+(L_{opt})}{\beta^+(0)} + \alpha_p \ln \frac{\beta^+(L_{opt})}{\beta^+(0)} = -\alpha_s + \alpha_s U q_0 + \alpha_s \ln \frac{1}{U q_0} \quad (50)$$

In order to simplify this equation such that known parameters are involved (mirror reflectivities), at $z=0$ and $z=L_{opt}$ the next boundary conditions are satisfied

$$\beta^+(0) = r_1 \beta^-(0) \quad (51)$$

$$\beta^-(L_{opt}) = r_2 \beta^+(L_{opt})$$

Where r_1 and r_2 are (respectively) the HR and OC reflectivities. Because both signals experience the same gain, the product of $\beta^+(L_{opt}) = \beta^+(0)e^{gL_{opt}}$ and $\beta^-(L_{opt}) = \beta^-(0)e^{-gL_{opt}}$ gives $\beta^+(L_{opt})\beta^-(L_{opt}) = \beta^+(0)\beta^-(0)$; the next constant may be defined for any length (See Fig. 7)

$$\beta^2 = \beta^+(z)\beta^-(z) \quad (52)$$

Then, from $\beta^+(0)\beta^-(0) = \beta^+(L_{opt})\beta^-(L_{opt})$ and using the boundary conditions the single-pass gain becomes

$$\frac{\beta^+(L_{opt})}{\beta^+(0)} = \frac{1}{\sqrt{r_1 r_2}} \quad (53)$$

That introduced in equation (50) and solving for the intra-cavity power signal, we obtain a numerical value as

$$p = -\frac{\alpha_p \ln \sqrt{r_1 r_2} - \alpha_s (1 - U q_0 + \ln U q_0)}{\alpha_p U' \ln \sqrt{r_1 r_2}} \quad (54)$$

And the optimal length may be obtained by re-arranging equation (48) as

$$\frac{1+p+q}{q} dq = -\alpha_p (U' p + 1) dz \quad (55)$$

That integrated over the same limits gives the value of the optimal length for maximum efficiency as

$$L_{opt} = \frac{\ln U q_0 (p+1) + q_0 - 1/U}{\alpha_p (U' p + 1)} \quad (56)$$

For example, two estimations of optimal length as function of pump power are given in Figure 9 for a Ho³⁺-doped ZBLAN fiber laser oscillating at $\lambda_s \approx 1194$ nm (see the emitting spectrum in Fig. 8) with 5000-ppmwt concentration, 7.5-micron core diameter and $\tau = 3.5$ ms. In Fig. 9(a) the pump was $\lambda_p = 1117$ nm and the stars correspond to the cavity lengths of the experiments; then, the lengths used were optimum for very low powers between 100 and 200 mW.

Fig. 9(b) corresponds to an estimation when pumping at $\lambda_p = 1175$ nm; here the 84-cm cavities, one with HR=0.04 (r_1) and OC=0.04 (r_2) and the other with HR=1 and OC=0.04, are good for very low powers; but the 1.5-m cavity is optimum for powers above 1W.

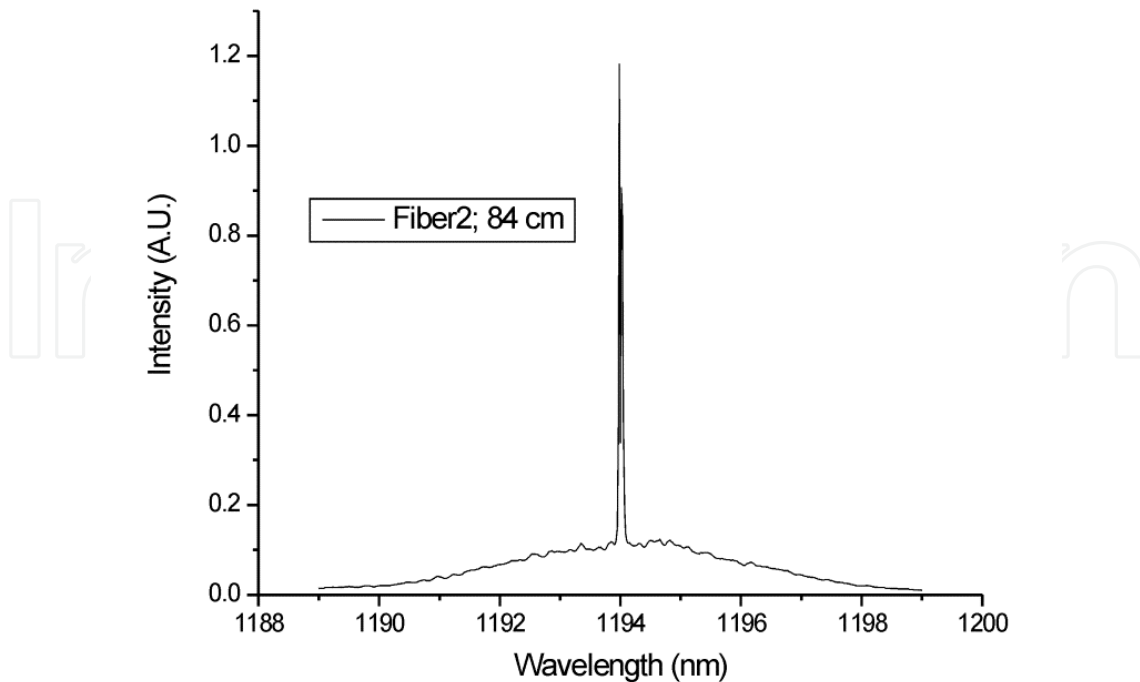


Fig. 8. Typical emission spectrum of a Ho^{3+} -doped fiber laser when pumped at 1117 or 1175 nm.

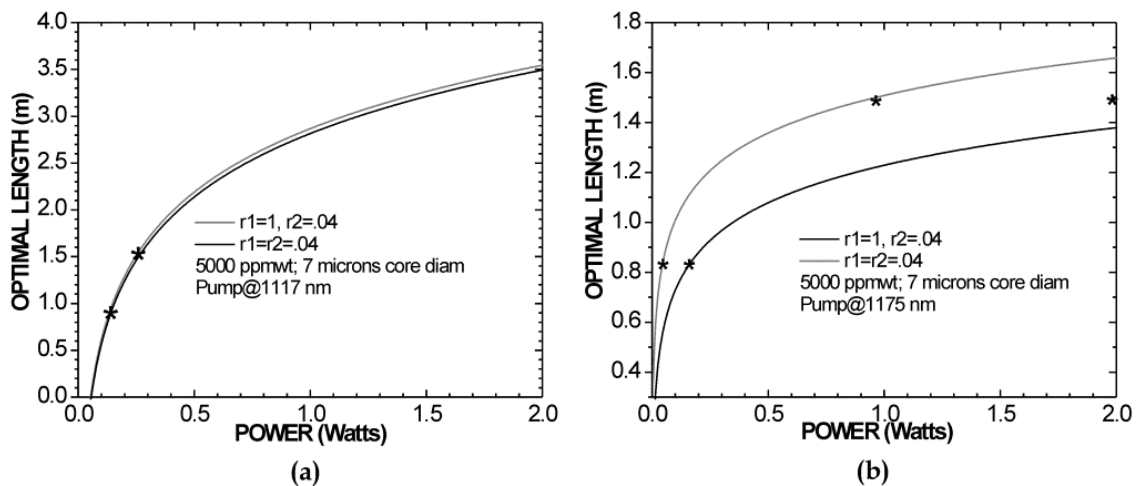


Fig. 9. Optimal fiber laser length (a) 1117-nm pump (b) 1175-nm pump.

The model has been proven with the fiber lasers mentioned at the beginning of this section and presents good agreement with the experimental results.

4. Other rare-earth fiber devices

In this section, two relatively modern applications of REDF's are described, both based on the upconversion phenomenon that is responsible of multi-photon absorption. These

devices depend on the development of special types of glasses that extended the possibilities for light converters.

4.1 Upconversion fiber lasers and amplifiers

After the parallel development of Nd³⁺-doped systems emitting at 1064 nm and laser diodes (LD's) at ~809 nm, most FL research has been devoted to 980-nm pumped Er³⁺-doped fiber lasers (EDFL's) and amplifiers (EDFA's) operating in the highest transparency of optical fibers, around 1550 nm, most specifically the C-Band at 1530-1565 nm (Digonnet, 2001). At present, the necessity of more optical channels has attracted interest for the Er³⁺ 1565- 1625 nm (L-Band) and the Tm³⁺ 1460-1530 nm (S-Band). Although somehow mentioned, there are in general, two main facts that limit operation of silica-based fiber lasers to operate from ~800 nm to ~2200 nm. The main one is pump availability. The most mature semiconductor technology that is in the market includes laser diodes emitting in the ~800-850 nm, ~900-980 nm and ~1500-1600 nm regions. Besides, there is a quantum rule that establishes that, in general, the lowest energy excited states of RE³⁺ are the most stable. In other words, one ion that is excited to the highest energy levels will make quick transitions down to the low energy levels. During their multi-step decay, they will stay shorter times at the superior levels and, in general, the lifetime will increase as it approaches the lowest energy levels. Then, in high phonon-energy materials such as silica, the metastable levels are the low-energy ones that are resonant with shorter wavelengths. Because of this, the VIS-UV regions started being explored until the development of low-energy phonon materials such as the fluoride-zirconium based or the tellurites. On these, two adjacent energy levels are less *thermally-connected* and as a consequence the multi-phonon decay rate is much lower. Then, the accumulation of population in all the levels (especially the highest) is more probable. In addition, the lifetimes increase and even the highest energy levels are metastable. Optical glasses such as ZBLAN or tellurites are efficient in subsequently absorbing two or more low-energy photons to produce another with higher energy. This up-conversion phenomenon permits the conversion of two or more IR photons into a UV-VIS one. At present, VIS-UV laser diodes deliver quite modest powers. Although this is the ideal source for any laser wavelength they present several challenges because material damage occurs at modest powers. A general rule for laser diodes is that good beam shape (single-mode and quasi-circular) is associated to low power of some milliwatts whereas high power LD's usually consist of an arrangement of low power ones or an arrangement of highly-rectangular end-emitting LD's. An improvement from the oldest technology of electrically exciting gases like Argon, Xenon or Neon is represented by frequency doubling or tripling solid state lasers such as the Nd:YAG or Nd:YVO₄. In general, producing low-energy photons from high-energy ones is easier because the conservation law of energy tell us that *the energy delivered by a system is equal to the energy absorbed minus the energy lost during the conversion*. This is not the case when producing high-energy photons departing from low energy ones; in this case, more than one photon is necessary.

Several upconversion fiber lasers in the UV-VIS region have been demonstrated; Pr³⁺:ZBLAN for example covers RGB regions that are important for laser displays; Nd³⁺ has produced 380 and 410 nm; Ho³⁺ and Er³⁺ green; Tm³⁺ blue (450 and 480 nm), UV (284 nm) and red (650 nm) (Funk & Eden, 2001; El-Agmy, 2008). Other important applications include those in which small spot size represents high-density storage, high resolution printing and fine lithography; although strong light-matter interactions makes them important for surgery being the most common eye-surgery; other applications extent to UV-curing of polymers

and epoxies, sterilization of medical instruments, etc. Blue fiber lasers in particular are important for undersea optical communications because cold water from the sea is transparent in the 470-500 nm region.

4.2 Light controlling light fiber attenuators

Although the activation of the absorption in the upper states has been reported before most authors have not exploited the use of this phenomenon for photonic devices other than optical sources. Recently, we have demonstrated that it is possible to attenuate or modulate a guided beam inside an optical fiber by another beam (Mejia & Pinto, 2009). Attenuation in optical fibers is usually realized by using bulk attenuators (or modulators) between two fibers which, in general, implies extracting light from one fiber, attenuate (or modulate) and then coupling back to the fiber link. This is basically a bulky approach that as such has the disadvantage of presenting high insertion losses. One of the simplest all-fiber approaches consists on physically deforming an optical fiber to induce the losses. It implies fiber fatigue and hence limitations in the life of the device. Purely photonic approaches in which one beam of light controls another one have been recently demonstrated and have still several limitations such as non-transparency recovery.

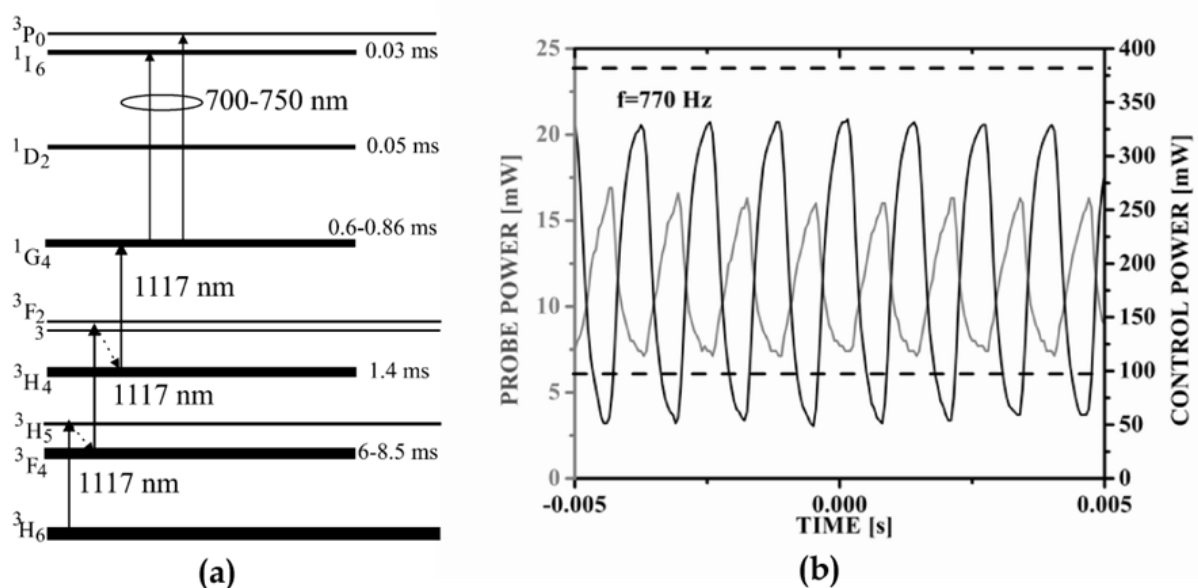


Fig. 10. (a) Energy levels involved in 700-750 nm attenuation by a control 1117-nm signal (b) Traces of probe signal in gray color (use left scale) and control (black with scale on the right).

An energy-level diagram that displays the transitions involved in our experiments is depicted in Figure 10 (a). An initial 1117-nm photon is absorbed by a Tm ion in the transition ${}^3\text{H}_6 \rightarrow {}^3\text{H}_5$ and from ${}^3\text{H}_5$ the ion rapidly decays non-radiatively to the high lying ${}^3\text{F}_4$ state ($\sim 6-8.5$ ms); a second photon populates the ${}^3\text{F}_{3,2}$ short lived states, from where the ions suffer a fast relaxation to the ${}^3\text{H}_4$ level (~ 1.4 ms), and *third-step* photons populate ${}^1\text{G}_4$ that is also metastable ($\sim 0.6-0.86$ ms). In this way, the transitions ${}^1\text{G}_4 \rightarrow {}^3\text{P}_0$ and ${}^1\text{G}_4 \rightarrow {}^1\text{I}_6$ become active and their band overlapping absorbs in the 700-750 nm interval. In this way, a 725-nm probe signal was controlled as guided through an optical fiber. Figure 10 (b) shows both signals; note that the operation is superior to 700 Hz. The fiber was a ~ 45 -cm ZBLAN fiber, doped with 2000 ppmwt of Tm^{3+} , 3- μm core diameter. The system was capable of 79-%

attenuating 700 mW of 711.2-nm probe signal by co-propagating 800 mW of control signal. The system perfectly operated as an optical inverter up to 200 Hz. The theoretical limit for working as an optical inverter was ≈ 1100 Hz. The dashed horizontal lines in the figure are the maximum and minimum reached by the probe at low frequencies. Because the phenomenon responsible for the attenuation (upconversion) depends on the time taken to absorb three photons, the induced attenuation is practically instantaneous. Then, the response of the system is imposed by 1G_4 -lifetime. This system may be important in those applications requiring uniform attenuation of all the cross section of a beam because it attenuates the whole signal coupled in the fiber core at once. Other opportunities are optically-controlled Q-switching of lasers because loss-modulations within 5-10% are typical. Because the system modulated at least 37% above 700 Hz, smaller modulations imply an increase of operating frequency. As the control signal in a commercial device of this type would be produced from a laser diode, the non-mechanical and purely photonic nature of the system (driven by low-voltage electronics) makes it robust. An additional advantage of the scheme is that it is polarization independent.

5. Conclusion

Rare-earth doped optical fibers had played a prominent role in laser development. Their geometry, that usually includes a circular core, has proven to be among the main reasons to choose them as laser converters. The devices based on these fibers are very compatible with the optical fiber infrastructure that covers the globe. Laser efficiencies have over-passed the dreams of first laser researchers; their powers have scaled up in such a way that also the dreams of first fiber-laser researchers has been over-passed; quite modest cooling systems for REDFL's have made possible the production of kilowatts of optical power. In telecommunications the optical amplifiers made possible the high speed regeneration of optical channels within the optical fiber networks and the amplification windows have expanded. Other devices like sensors, broadband sources and optical attenuators are still to be developed because new types of optical fibers (the photonic crystal type, for example) improve their performance. Because these devices depend on diode laser development, every time a new diode laser appears, their possibilities increase.

6. Acknowledgment

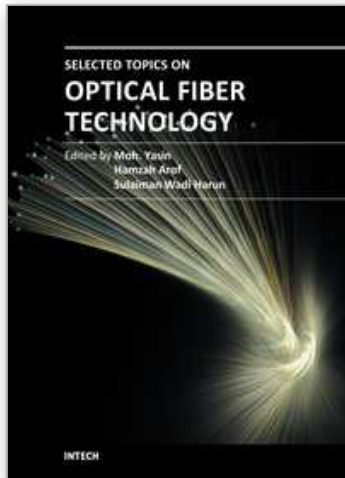
This work was supported by CONCYTEG and CONACYT-México.

7. References

- Agrawal, GP (1989). *Nonlinear Fiber Optics* (Second Edition), Academic Press, ISBN 0-12-045142-5, California, USA
- Castrellón-Urbe, J. & García-Torales, G. Remote Temperature Sensor Based on the Up-Conversion Fluorescence Power Ratio of an Erbium-Doped Silica Fiber Pumped at 975 nm. *Fiber and Integrated Optics*, Vol. 19, No. 4, (July 2010), pp. 272-283, ISSN 1096-4681
- Desurvire, E. (1994). *Erbium-Doped Fiber Amplifiers: principles and applications* (First Edition), Wiley-Interscience, ISBN 0-471-58977-2, New York, USA
- Digonet, M. (2001). *Rare-Earth-Doped Fiber Lasers and Amplifiers* (Second Edition), Marcel Dekker, ISBN 0-8247-0458-4, New York, USA

- El-Agmi, RM. Upconversion CW Laser at 284 nm in a Nd:YAG-Pumped Double-Cladding Thulium-Doped ZBLAN Fiber Laser, *Laser Physics*, Vol. 18, No. 6, (June 2008), pp. 803-806
- Funk, D. & Eden, G. (2001). Visible Fluoride Fiber Lasers, In: *Rare-Earth-Doped Fiber Lasers and Amplifiers*, Michael J.F. Digonnet, (Ed.), 171-242, Marcel Dekker, ISBN 0-8247-0458-4, New York, USA
- Lucas, J. (1989). Fluoride glasses. *Journal of Materials science*, Vol. 24, No.1, (January 1989), pp. 1-13, ISSN 0022-2461
- Luu-Gen, H. & Chen-Ke, S. The Structural Investigation of a ZBLAN Glass by Vibrational Spectroscopy, *Chinese Journal of Physics*, Vol. 34, No. 5, (October 1996), pp. 1270-1275
- Mejía, E. & Pinto, V. Optically controlled loss in an optical fiber, *Optics Letters*, Vol. 34, No. 18, (September 2009), pp. 2796-2798
- Miniscalco, W. (2001). Optical and Electronic Properties of Rare Earth Ions in Glasses, In: *Rare-Earth-Doped Fiber Lasers and Amplifiers*, Michael J.F. Digonnet, (Ed.), 17-105, Marcel Dekker, ISBN 0-8247-0458-4, New York, USA
- Pauling, L. (1988). *General chemistry* (First Dover Edition), Dover Publications, ISBN 0-486-65622-5, New York, USA
- Po, H.; Snitzer, E.; Tumminelli, R.; Zenteno, L.; Hakimi, F.; Cho, N. & Haw, T. (1989). Double Cladd High Brightness Nd Fiber Laser Pumped by GaAlAs Phased Array, *proceedings of Optical Fiber Communication Conference*, ISBN 978-9999904467, Houston, Texas, USA, February 1989
- Quin, L., Shen, ZX., Low, BL., Lee, HK., Lu, TJ., Dai, DS., Tang, SH., & Kuok, MH. Crystallization Study of Heavy Metal Fluoride Glasses ZBLAN by Raman Spectroscopy, *Journal of Raman Spectroscopy*, Vol. 28, No. 5, (July 1997), pp. 495-499
- Siegman, A. (1986). *Lasers* (First Edition), University Science Books, ISBN 0-935702-11-5, Mill Valley, California, USA

IntechOpen



Selected Topics on Optical Fiber Technology

Edited by Dr Moh. Yasin

ISBN 978-953-51-0091-1

Hard cover, 668 pages

Publisher InTech

Published online 22, February, 2012

Published in print edition February, 2012

This book presents a comprehensive account of the recent advances and research in optical fiber technology. It covers a broad spectrum of topics in special areas of optical fiber technology. The book highlights the development of fiber lasers, optical fiber applications in medical, imaging, spectroscopy and measurement, new optical fibers and sensors. This is an essential reference for researchers working in optical fiber researches and for industrial users who need to be aware of current developments in fiber lasers, sensors and other optical fiber applications.

How to reference

In order to correctly reference this scholarly work, feel free to copy and paste the following:

Efraín Mejía-Beltrán (2012). Rare-Earth Doped Optical Fibers, Selected Topics on Optical Fiber Technology, Dr Moh. Yasin (Ed.), ISBN: 978-953-51-0091-1, InTech, Available from:

<http://www.intechopen.com/books/selected-topics-on-optical-fiber-technology/rare-earth-doped-optical-fibers>

INTECH
open science | open minds

InTech Europe

University Campus STeP Ri
Slavka Krautzeka 83/A
51000 Rijeka, Croatia
Phone: +385 (51) 770 447
Fax: +385 (51) 686 166
www.intechopen.com

InTech China

Unit 405, Office Block, Hotel Equatorial Shanghai
No.65, Yan An Road (West), Shanghai, 200040, China
中国上海市延安西路65号上海国际贵都大饭店办公楼405单元
Phone: +86-21-62489820
Fax: +86-21-62489821

© 2012 The Author(s). Licensee IntechOpen. This is an open access article distributed under the terms of the [Creative Commons Attribution 3.0 License](#), which permits unrestricted use, distribution, and reproduction in any medium, provided the original work is properly cited.

IntechOpen

IntechOpen